Temperature Factor Effect on Separated Flow Features in Supersonic Gas Flow

V. Ya. Neyland, L.A. Sokolov, and V.V. Shvedchenko

Abstract The effect of the temperature factor (body temperature ratio to the stagnation temperature of external flow) on the separated flow features has been investigated in the supersonic gas flow near the concave angle. The strong effect of the temperature factor on the separated zone length and on the corresponding aerodynamic performances was revealed. It was shown that, if the angle is big enough, such flow cannot be described by free interaction theory, i.e. by triple deck theory.

Nomenclature

U	Velocity
p	Pressure
ρ	Density
T	Temperature
H	Total enthalpy
M	Mach number
Re	Reynolds number
Pr	Prandtl number
δ	Boundary layer thickness
ℓ	Boundary layer length
μ	Coefficient of viscosity
ω	Power in viscosity law
g_w	Temperature factor
γ	Specific heat ratio
x	Longitudinal coordinate
y	Normal coordinate
Δx	Separation zone length
θ	Flare angle

V.Y. Neyland (✉)
TsAGI, Zhukovsky, Moscow region, 140180, Russia, E-mail: Neyland@tsagi.ru

A.F. Hegarty et al. (eds.), *BAIL 2008 - Boundary and Interior Layers.*
Lecture Notes in Computational Science and Engineering,
DOI: 10.1007/978-3-642-00605-0,

1 Introduction

The investigation of separated flow in viscous supersonic flow near a flat plate caused by the rear part of the flat plate deviating by an angle θ is an important task in the development of separated flow theory. It is also significant for the applications when temperature factor becomes small in the flight with high supersonic speed. It is important that, when testing models in the wind tunnel, the temperature factor may considerably differ from its flight value (Table 1). It can lead to the considerable deviations of the aerodynamic performances and heat fluxes in the wind tunnel from those in the actual flight. So far, the flow over the flat plate with deviated rear part was investigated in many theoretical and experimental works. A review of the results is given in [1–4].

During the first decades, theoretical investigations of these flows were divided into two directions. For the developed separated flows included the pressure "plateau" zone method with the criteria of Chapman–Korst [5, 6] was used. Later it was shown [7] that the criteria method of Chapman (for laminar flows) corresponds to the first approach of the strict asymptotic theory for Navier–Stokes equation. For small separated zones and zones of incipient separation without developed pressure "plateau" area, another approach based on the integral equations of the boundary layer was more appropriate.

After the development of free interaction theory [8–11] (usually called "triple deck" outside of Russia) the other multilayer solutions were obtained [7, 12].

Within asymptotic theory, the calculation of the flow near "compression corner" with an angle of $\theta \sim \mathrm{Re}^{-1/4}$ was performed by many authors [11–14]. Recently the author of [13] assumed that solution of this task within free interaction theory only exists up to some critical value of $\theta/\mathrm{Re}^{-1/4}$. Later similar calculations were performed in [14] more carefully and the authors showed that the conclusions of [13] were caused by a wrong calculation method. But they referred to the asymptotic reattachment theory developed in [7] which does not contain singularities. It should be noted that the applicability of the free interaction theory is a complicated matter, although the criticism of the numerical results of [13] by authors of [14] is, may be, correct.

Table 1 Temperature factor in flight ($T_w \sim 1{,}000$ K) as compared with that in wind tunnel

H, km	M = 10	15	20	25
40	0.193	0.0858	0.048	–
50	0.182	0.0807	0.046	–
60	0.196	0.0807	0.045	–
70	0.227	0.101	0.057	0.036

M	T_0	g_w
3–5	750	0.4
6–10	1,075	0.279
10, 12, 14, 18	2,600	0.115

The present article is based on two methods: qualitative analytical investigation of flow physical features and numerical investigation of the Navier–Stokes equations. The investigations assume that the flow is laminar everywhere.

2 Analytical Investigation

Let us consider supersonic flow over a flat plate at zero angle of attack. The rear part of the plate is deflected by an angle θ (Fig. 1). The angle θ, Mach number M and Reynolds number Re are so that the separated zone appears upstream of the angle.

Let us first consider the small separated zones and zones of arising separation. For this purposes it is convenient to use the method described in the monographs [15,16]. This approach was used in [8,9] for the free interaction theory development which later was proposed in [10] under the name of triple deck and using a slightly different way.

Thus, let us consider flow in a small vicinity of the separation point of the boundary layer (Fig. 1). Let a small pressure difference $\Delta p/p \ll 1$ be applied to the flow. In the major part of the boundary layer, where the longitudinal component of the velocity U is of the same order as the outer flow velocity Ue, we can use equation of the longitudinal momentum, state equation and relation $\rho_e u_e^2 \sim p$ to obtain

$$\rho U U_x \sim p_x, \quad \rho_e U_e \Delta U \sim \Delta p, \quad \frac{\Delta\rho}{\rho} \sim \frac{\Delta p}{p}.$$

Then, in this part of the boundary layer (area 2 in Fig. 1), because of the continuity equation, the disturbed streamline thickness assessment has the following form

$$\frac{\Delta\delta}{\delta_0} \sim \frac{\Delta p}{p},$$

where δ_0 is the typical value of boundary layer thickness upstream of the interaction area.

Near the wall, because of the boundary condition, in the undisturbed boundary layer there is always area 3 where the dynamic pressure will be of order Δp. It is

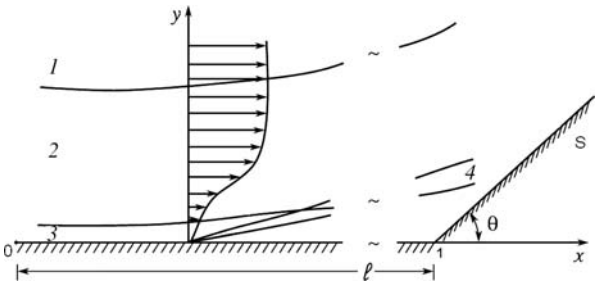

Fig. 1 Flow scheme

only true near the separation point, because far from it the $\Delta\, p$ can be balanced by viscous forces and the task becomes linear.

Thus, for area 3 we obtain the assessment

$$\rho_3 U_3^2 \sim \Delta p. \tag{1}$$

In area 3, using the relationship for the velocity profile in the undisturbed boundary layer, we can obtain assessment

$$\frac{U_3}{U_e} \sim \frac{\delta_3}{\delta_0}. \tag{2}$$

In area 3 the flow upstream of the separation point is performed against inadvertent pressure difference $\Delta p > 0$ by viscous forces, i.e.

$$\frac{\rho\, U_3^2}{\Delta x} \sim \mu_3 \frac{U_3}{\delta_3^2}. \tag{3}$$

Due to (1) the thickness of area 3 varies as the undisturbed value, then (1) and (2) result in

$$\frac{\delta_3}{\delta_0} \sim \frac{U_3}{U_e} \sim \sqrt{\frac{\Delta p}{p}} \gg \frac{\Delta p}{p} \sim \frac{\Delta \delta_2}{\delta_0}.$$

Thus, in the first approach, the total variation of the boundary layer momentum thickness is produced by area 3.

This fact together with linear theory of supersonic flows (Ackeret formula) leads to the last estimate

$$(\mathrm{M}_e^2 - 1)^{1/2} \Delta p \sim \rho_e U_e^2 \frac{\delta_3}{\Delta x}. \tag{4}$$

To determine scales of the disturbed values Δx, Δp, U_3, δ_3 we get four equations (1)–(4). They give us estimates of all the required values

$$\Delta x \sim \ell \mathrm{Re}^{-3/8}, \quad \frac{\Delta p}{p} \sim \mathrm{Re}^{-1/4}, \quad \frac{U_3}{U_e} \sim \frac{\delta_3}{\delta_0} \sim \mathrm{Re}^{-1/8}. \tag{5}$$

The angle θ which produces the separation of the boundary layer has the order of the value $\mathrm{Re}^{-1/4}$ (ℓ is the boundary layer length upstream of the separation point).

Using the estimates (5) we can develop asymptotic theory of Navier–Stokes solution for the small separation zones at $\mathrm{Re} \to \infty$.

Let us consider this task for the flows with high supersonic speeds and small temperature factor using limit

$$\mathrm{Re} \to \infty,\ \mathrm{M} \to \infty,\ g_w = \frac{H_w}{H_e} \to 0,$$

where H is total enthalpy, indexes e and w correspond to the parameter values at the outer boundary of the boundary layer and the wall respectively.

Let us assume, that the interaction of the non-viscous flow with the boundary layer is small up to the separation point. Then

$$\delta_0/\ell \sim \left(\frac{\mu_0}{\rho_0 U_e \ell}\right)^{1/2},\ \mathrm{M}_e\delta_0/\ell \ll 1.$$

In the major part of the boundary layer (area 2 in Fig. 1) the gas temperature will be of the order of the total temperature T_0 [17], $\rho_2 \sim \rho_0 \sim \rho_e/M_e^2$, $\mu_2 \sim \mu_0$, where ρ_0, μ_0 are the density and viscosity at $T = T_0$.

Friction and heat flux to the wall maintain their orders of the value in the whole boundary layer, i.e.

$$\left(\mu\frac{dU}{dY}\right)_{y\to 0} \sim \mu_0\frac{U_e}{\delta_0};\quad \left(\mu\frac{dg}{dy}\right)_{y\to 0} \to \mu_0\frac{1}{\delta_0}.$$

Then the velocity and enthalpy profiles near the body surface will be (neglecting the inessential constants):

$$g \sim \left(g_w^{\omega+1} + \frac{y}{\delta_0}\right)^{1/(\omega+1)},\ \frac{U}{U_e} \sim \left(g_w^{\omega+1} + \frac{y}{\delta_0}\right)^{1/(\omega+1)} - g_w. \tag{6}$$

Depending on the relationship of g_w and the disturbed pressure amplitude $\Delta p/p$, using (6) we can get profiles in the area 3

$$g_w^{\omega+1} \gg \frac{\delta_3}{\delta_0} \qquad g_3 \sim g_w,\ \frac{U_3}{U_e} \sim \frac{1}{g_w^{\omega}}\frac{\delta_3}{\delta_o} \tag{7}$$

$$g_w^{\omega+1} \ll \frac{\delta_3}{\delta_0} \qquad g_3 \sim \left(\frac{\delta_3}{\delta_0}\right)^{1/(\omega+1)},\ \frac{U_3}{U_e} \sim \left(\frac{\delta_3}{\delta_0}\right)^{1/(\omega+1)}. \tag{8}$$

Let us consider regime (7). Near the separation point

$$\Delta p \sim \rho_3 U_3^2,\quad \frac{\delta_3}{\delta_0} \sim g_w^{(1+2\omega)/2}\cdot\left(\frac{\Delta p}{p}\right)^{1/2},\ \frac{U_3}{U_e} \sim g_w^{1/2}\left(\frac{\Delta p}{p}\right)^{1/2}. \tag{9}$$

The thickness of the area with non-linear disturbances (area 3, $\Delta\delta_3 \sim \delta_3$) will be of a greater order than that of the area 2 $\Delta\delta_2$ if the following condition is valid

$$g_w^{(1+2\omega)/2}\sqrt{\frac{\Delta p}{p}} \gg \frac{\Delta p}{p} \to \frac{\Delta p}{p} \ll g_w^{1+2\omega}. \tag{10}$$

Then, using Ackeret formula (4) for the area 1 (the disturbed part of the external non-viscous flow) we get an estimate for the length of the disturbed flow Δx

$$\frac{\Delta x}{\ell} \sim \frac{\mathrm{M}_e\delta_0}{\ell}\cdot\sqrt{\frac{g_w^{1+2\omega}}{\Delta p/p}}. \tag{11}$$

It shows that as g_w decreases, $\Delta x/\ell$ decreases also.

Let us obtain an assessment for the critical pressure differential assuming, as usual, that the viscous and inertial members are of the same order in the Navier–Stokes equations.

$$\frac{\rho_3 U_3^2}{\Delta x} \sim \mu_3 \frac{U_3}{\delta_3^2}; \quad \frac{\Delta p}{p} \sim \left(\mathrm{M}_e \frac{\delta_0}{\ell}\right)^{1/2}. \tag{12}$$

Thus, when decreasing g_w at fixed deflection angle of the plate rear part, the separation zone length decreases (11).

Further decrease of g_w violates conditions (7) and (10). Now, let us assume that

$$\frac{\delta_3}{\delta_0} \sim \frac{\Delta\delta_2}{\delta_0} \sim \frac{\Delta p}{p} \sim g_w^{1+2\omega}. \tag{13}$$

Then, using Ackeret formula in the form of $\Delta p/p \sim \mathrm{M}_e \delta_2/\Delta x$ we get assessment for the action Δx

$$\Delta x \sim \mathrm{M}_e \delta_0. \tag{14}$$

The relations (9) are true as long as area 3 remains almost isothermal ($g_w^{\omega+1} \gg \delta_3/\delta_0$).

Having assessment (13), let us estimate the critical pressure differential at this regime, using the first estimate of (12)

$$\frac{\Delta p}{p} \sim \left(\mathrm{M}_e \frac{\delta_0}{\ell}\right)^{2/3} g_w^{-2(\omega+1)/3}. \tag{15}$$

The estimate shows that at fixed length of the disturbed area (14) decrease of g_w leads to the increase of the critical pressure difference (15). It means that at fixed angle of deflection of plate rear part the separated area length will also decrease.

And finally, if the isothermal condition of area 3 (7) is violated, estimate (14) for Δx will remain because $\Delta\delta_2 \gg \delta_3$. The estimate for g_3, U_3/U_e, and δ_3/δ_0 will have the form of (8). Then for the critical value of the pressure difference which produces separation initiation in the area 3 the following assessment is obtained, using equations (1) and (3)

$$\frac{\Delta p}{p} \sim (\mathrm{M}_e \delta_0/\ell)^{1/(2\omega+1)}.$$

This estimate is true for all small g_w when equation (8) is valid.

Now, let us investigate the effect of g_w on the separation zone length at a slightly higher value of θ when the zone appears with almost constant pressure but mixing layer at the outer boundary of the separated zone is still much thinner than the boundary layer separated from the body surface. To get the necessary assessment let us assume that the Korst–Chapman condition [5] or asymptotic attachment theory [7] is true.

In this case the following relationship must be valid $\theta_{inc} \ll \theta \ll 1$. The upper limitation provides fulfilment of the condition $\delta_4 \ll \delta_0$, where θ_{inc} is the angle at which mixing layer 4 leaves the body after separation.

At $\theta_{inc} \sim \theta$ we come back to the free interaction theory considered above (for example, at $\theta \sim \mathrm{Re}^{-1/4}$ and $g_w \sim 1$ the separation zone length Δx is determined by (5) according to free interaction theory (triple deck)).

At $\theta \gg \theta_{inc}$ friction forces acting on the gas along dividing streamline lead to the dynamic pressure increase thus providing the possibility to counteract pressure rise in the attachment area. The Korst–Chapman condition [5, 6] may be written as

$$\rho_4 U_4^2 \sim \Delta p, \quad \frac{\Delta p}{p} \sim \mathrm{M}_e \theta. \tag{16}$$

Here, index 4 designates parameters value at dividing streamline in the mixing layer. As $\delta_4 \ll \delta_0$ i.e. the separated zone is short, $\Delta x/L \ll 1$, so $\rho_4 \sim \rho_w$. Further, we must estimate the rate of $U_4(\Delta x)$ increase.

In the mixing layer 4 the acceleration occurs due to longitudinal momentum transfer when friction forces act on streamlines of the separated boundary layer. Thus, we can write down the following conditions

$$\frac{U_4}{\delta_4} \sim \frac{U_e}{g_w^{\omega} \delta_0}; \quad \frac{\rho_4 U_4^2}{\Delta x} \sim \mu_4 \frac{U_4}{\delta_4^2}. \tag{17}$$

In (17) the first condition corresponds to the conservation of friction stress value in area 4 to its value in the separated boundary layer, where $U \sim U_e$, thickness δ_0, and $\mu_4/\mu_0 \sim g_w^{\omega}$. The second condition in (17) is balance of orders of value of viscous and inertial members in the longitudinal momentum equation.

Resolving (17) we obtain the estimates

$$\frac{\delta_4}{\delta_0} \sim g_w^{(1+2\omega)/3} \left(\frac{\Delta x}{\ell}\right)^{1/3}, \quad \frac{U_4}{U_e} \sim g_w^{(1+2\omega)/3} \left(\frac{\Delta x}{\ell}\right)^{1/3}. \tag{18}$$

Here, ℓ is boundary layer length up to the separation point, while Δx is the mixing zone length from the separation point to the attachment point. At $g_w \sim 1$ (18) corresponds to the known selfsimilar solution of Prandtl equation for the mixing layer between external flow with shear profile and stagnation zone. Now, using condition in the attachment zone (16) we get dependence of the separation zone length on θ and g_w

$$\frac{\Delta x}{\ell} \sim (\mathrm{M}_e \theta)^{3/2} \cdot g_w^{(1+2\omega)/2}.$$

Thus, the separation zone length decreases with g_w decreasing in this regime also.

3 Numerical Investigation

Numerical investigation was performed with the use of computer codes packet of numerical integration of Navier–Stokes equations by time-dependent method developed in TSAGI [18–20].

The initial boundary-value problem was solved by the integro-interpolation method (finite volume method). Implicit monotonic scheme of the type of Godunov [21] scheme and the approximate method of Roe [22] of solving the Riemann problem on break-up of arbitrary discontinuity were used in the approximation of the convection component of flow vectors in half-integer nodes. The principle of minimal derivates [23] was used for raising the order of approximation to second one in the case of interpolation of dependent variables to the face of elementary cell. A difference scheme of the type of central differences of the second order of accuracy was used in the approximation of the diffusion component of flow vectors on the face of elementary cell. The modified Newton–Raphson method was used for solving the nonlinear finite-difference equations. The set of linear algebraic equations was solved using the GMRES(k) method of minimal residuals [24].

The flow field near the two-dimensional compression corner protruding into the supersonic flow (Fig. 1) has been calculated at following parameters: Reynolds number based on a plate length up to the corner point $\mathrm{Re} = 10^6$, Mach number $\mathrm{M} = 5$, Prandtl number $\mathrm{Pr} = 2/3$, temperature factor $g_w = 10^{-3}/1$, specific heat ratio $\gamma = 5/3$, viscosity law $\mu \sim T^{\omega}(\omega = 0.5)$.

In the investigated area the coordinate origin coincides with the beginning of the non-deflected part of the plate, deviation point is located at $x = 1$, the end of the investigated area is located at $x = 5$.

At the left boundary the undisturbed flow was chosen. Upper boundary of the computed area was chosen so that the boundary conditions were also undisturbed external flow. Right boundary of the computed area was chosen so that error in soft boundary conditions did not effect on the solution in the vicinity of the separation zone. The condition of no-slip were chosen at the body surface. The special grid thickening at the plate beginning was performed to correctly follow the abrupt pressure gradient at the leading edge. It should be noted that errors at the leading edge does not effect on the solution downstream and dissipate quickly with distance from leading edge if the separation zone is not located near the leading edge.

Following the method of analytical grid development [20] the grid thickening near the body surface was performed with line number about 20–40% of the total number in the direction of the boundary layer thickness. It allowed one ensure high resolution of boundary layer near the body surface. This method of analytical grid is appropriate for small $\theta < 10°$ when the separation zone dimensions are small. It allows one cover the separation zone with a grid of necessary density and to simulate actual flow pattern.

The grid resolution in the area of abrupt pressure gradient in the attachment zone also strongly effects the quantity of the obtained results. The additional grid thickening in this area both in longitudinal and transversal coordinates is required. In the rest of the computation area the grid is quasi-uniform. The grid resolution in the

separation area does not strongly effect the flow pattern if separation does not start from the leading edge.

For angles $\theta = 10°, 20°$ the separation zone dimensions are much more than the boundary layer and the mixing layer thickness. In this case the method of analytical grid is not working. The issue may be in development of adaptive grids [25]. This method allows not only to get correct flow pattern but also to considerably decrease the required number of lines (for $\theta = 10°$). Sometimes ($\theta = 20°$) it is the only possible method to get solution.

With the task features in mind, the grids were used having one-dimension adaptation in the direction normal to the surface constructed by "equidistribution" method [26]. It allows one to fine solve the mixing layer and to check the solution on grids with different number of nodes. If the resolution and adaptation were correctly chosen the mixing layer position practically does not change when the number of grid nodes varies by 2–4 times. To get a final solution the adaptive iterations on the grids with small number of nodes were repeated many times until convergence was obtained. Then the solution was checked with number of grid nodes variation by 2–4 times. The solutions obtained with the use of analytical grids were unstable when the number of nodes increased. The maximum dimensions of the grids were $1{,}600 \times 200$ for $\theta = 10°, 20°$ and 800×200 for $\theta < 10°$. At this, the solutions were checked for convergence on different grids.

For big angles $\theta = 10°, 20°$ the grid resolution does not effect the mixing layer position but considerably changes flow pattern inside the separated zone.

4 Results

Figure 2 shows the pressure distribution along the x-axis on the corner surface. Pressure is normalized to $\rho_\infty U_\infty^2$ ($p_\infty/\rho_\infty U_\infty^2 = 1/\gamma \mathrm{M}^2 = 0.024$). On the plate surface ($\theta = 0$) at $x \sim 1$ the pressure becomes constant increasing as the temperature factor increases. For $\theta = 2.5°$ full attached flow occurs. For larger angles the separated flow occurs with the separated zone length increasing as both θ and temperature factor increase. When temperature factor increases the separation point moves to the left while the attachment point moves to the right. Temperature factor increase causes small pressure rise in the separated zone and increases pressure steps smoothness.

At $\theta = 2.5°$ separation starts near the leading edge, where the flow parameters vary considerably along the x-axis. The pressure steps smoothness decreases. Each value of the temperature factor corresponds to a certain value of pressure in the separation zone and to a certain x-coordinate of reaching maximum pressure. Inside the separation zone there were observed pressure oscillations caused by the development of vortices.

Figure 3 gives x-coordinates of the separation and attachment points where friction becomes zero. For small angles variation of full separation length Lx is caused (in equal proportions) by variation of its components Lx_1 and Lx_2 (upstream and

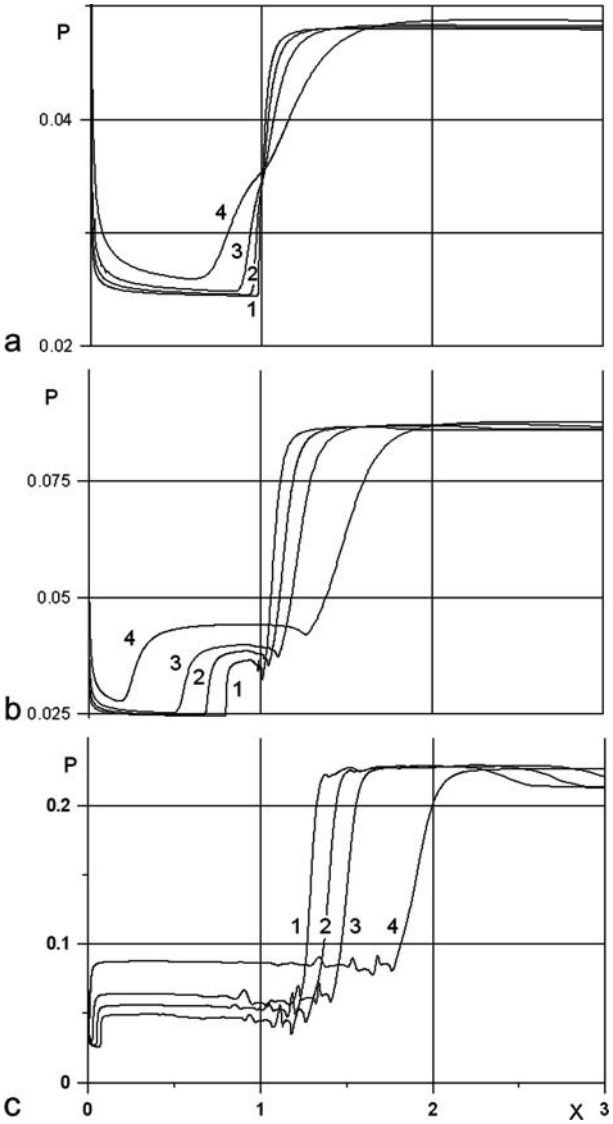

Fig. 2 Pressure distribution along x-coordinate of the corner $\theta^{\circ} = 5, 10, 20$ (**a, b, c**) at temperature factor $g_w = 0.001, 0.1, 0.3, 1$ (curves 1–4)

downstream of the corner correspondingly). For an angle $\theta = 20°$ $Lx_1 \sim 1$ and major variation of Lx is caused by Lx_2 component, i.e. by considerable displacement of the attachment point. For θ values increase of temperature factor leads to the separation zone length increase.

For angles $\theta = 10, 15, 20°$ the vortices were observed inside the separation zone (Fig. 4b–d) similar as to "bubble" in the work [27]. For angles $\theta = 5°, 7.5°$ (Fig. 4a) vortices were not discovered.

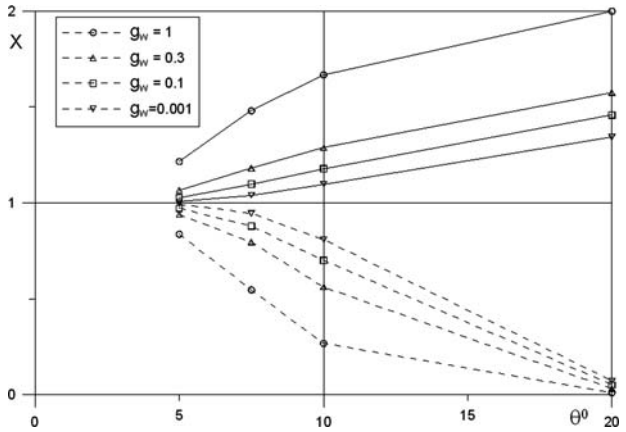

Fig. 3 Variation x-coordinates of separation (*dash line*) and attachment points (*solid line*) depending on angle θ and temperature factor $g_w = 10^{-3}$, 0.1, 0.3, 1

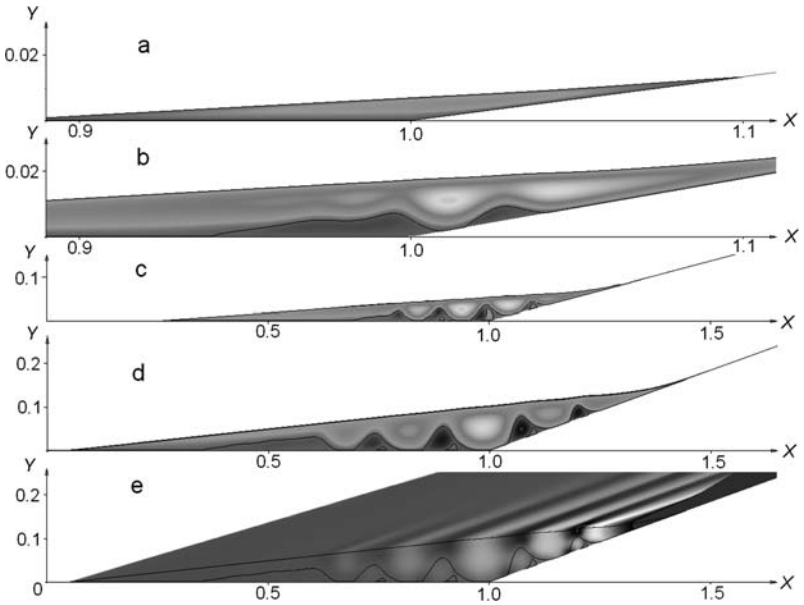

Fig. 4 Streamlines field for flow near the corner $\theta^\circ = 7.5$, 10, 15, 20 (**a**, **b**, **c**, **d**) and pressure (**e**) field $\theta^\circ = 20$ with temperature factor $g_w = 0.1$ (*solid line* corresponds to the zero streamline)

Investigation showed that, when the grid resolution was high enough, the large vortices sizes did not change. We should remark, that for $g_w = 1$ separation zone is large, thus, the grid step in the x-direction is 1.5–2 times greater than that for $g_w = 10^{-3}$–10^{-1}. That is why for $g_w = 1$ the vortices were only specified in details at a grid of 1,600 × 200 nodes. The grid of 800 × 200 did not give vortices details while at $g_w = 10^{-3} \cdots 10^{-1}$ vortices were seen quite clearly.

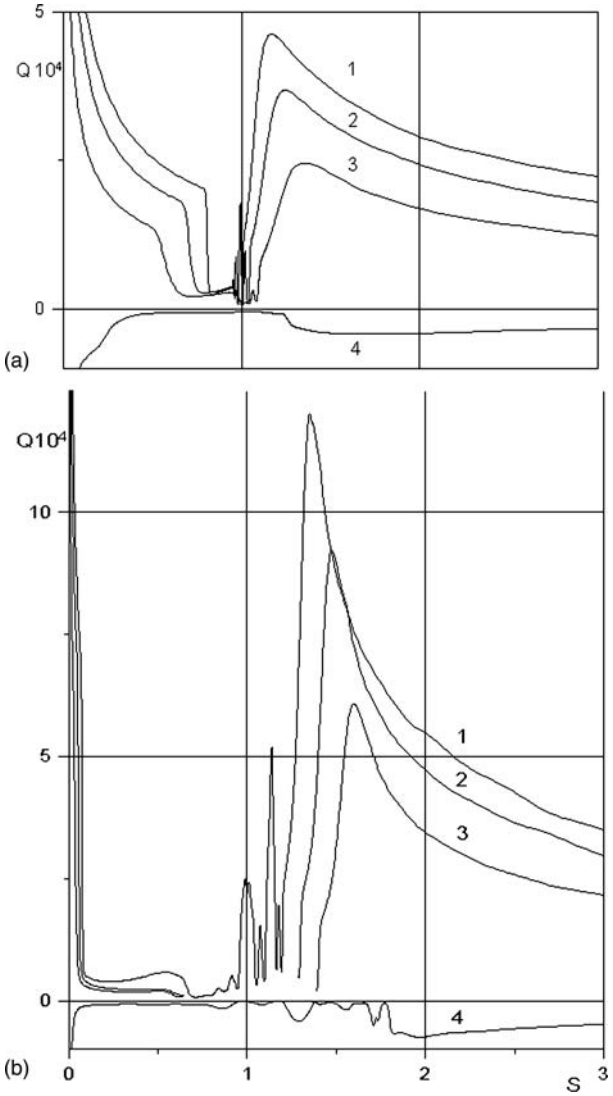

Fig. 5 Heat flux distribution along corner coordinate S for $\theta = 10$, 20 (**a**, **b**) at temperature factor $g_w = 0.001, 0.1, 0.3, 1$ (curves 1–4)

It is possible, that vortices development is caused by the separation of a viscous sublayer at the bottom of locally inviscid jet that flows out of the attachment zone of the main separation zone. In this case pressure across the separation zone becomes variable, i.e. $\partial p/\partial y \neq 0$ (Fig. 4b).

It is very interesting to investigate the effect of the temperature factor on the heat flux in the attachment zone (Fig. 5). The heat flux is normalized by $\rho_\infty U_\infty^3$. For all angles, when the temperature factor decreases maximum heat flux reaches its limit

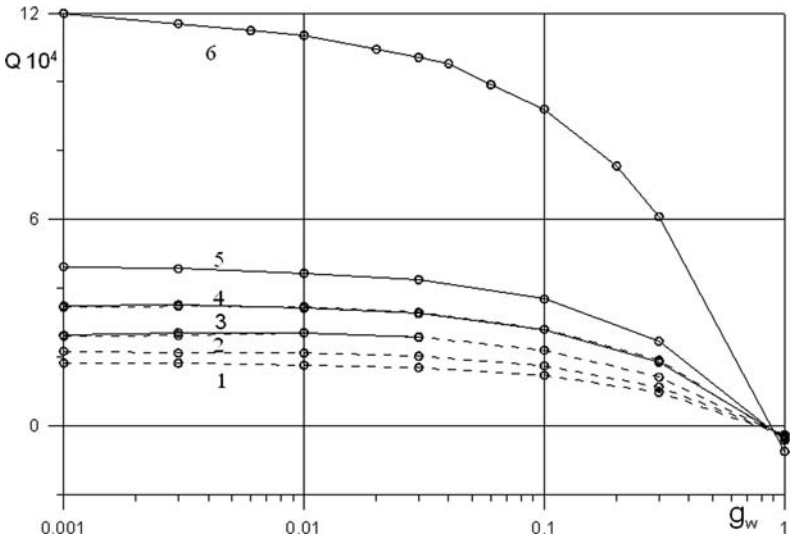

Fig. 6 Variation of maximum heat flux in the attachment zone depending on temperature factor g_w for angles $\theta^\circ = 0$, 2.5, 5, 7.5, 10, 20 (curves 1–6). *Solid line* corresponds to the adaptive grid, *dash line* –to the analytical grid

value (Fig. 6). For angles $\theta = 5°$, $\theta = 7.5°$ results are shown obtained both on analytical and adaptive grids, while for angles θ = 10, 20 - obtained on the adaptive grids only. For angles $\theta = 10,\ 20°$ (Fig. 5) there are heat flux splashes inside the separation zone (up to 40% of its maximum value at the attachment point) caused by vortices. For $\theta = 5°$ at $g_w \sim 10^{-2}$ and for $\theta = 7.5°$ at $g_w \sim 3\times10^{-3}$ there is weak maximum. It may be caused by calculation accuracy at small temperature factor when additional grid thickening is required because of the big density gradient near the surface. Such thickening, being small, does not effect on the global flow pattern in the separation zone, but is important for local heat flux modeling.

Big practical interest is the temperature factor effect on the effectiveness of flight controls of "ramp" type. Figure 7 gives the difference Δx between the pressure center locations in two cases: with g_w simulation and with pressure "step" obtained from inviscid corner flow. If there is a separation, we can specify two regions that effect the pressure center location: increased pressure zone inside the separation zone and increased pressure zone at the attachment point. For $\theta \leq 7.5°$ the input of the increased pressure zone inside the separation zone is practically balanced by the displacement to the right of the increased pressure zone at the attachment point.

So, there are two counteracting tendencies that determine the pressure center location depending on the temperature factor: (1) displacement to the left on the plate and (2) displacement of the attachment zone to the right. For small angles ($\theta < 7.5°$) displacement to the left on the plate overrides the displacement of the attachment zone to the right. For big angles ($\theta > 7.5°$) the input of high pressure

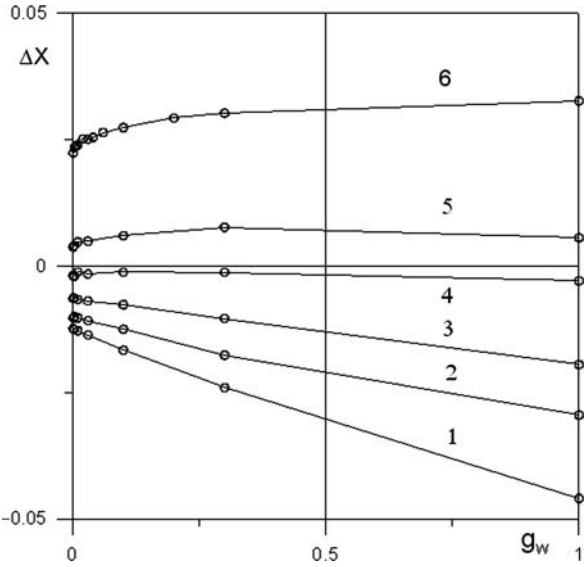

Fig. 7 Pressure center displacement ΔX as compared with position for inviscid flow near angle $\theta^\circ = 0, 2.5, 5, 7.5, 10, 20$ (curves 1–6) depending on temperature factor g_w

in the attachment zone on the pressure center position becomes significant and the pressure center moves to the right.

These results are given for the calculation area $x = [0,\ 5]$. For the ramp of actual geometry with small sizes similar effects may be observed, but it is a quite different task with different geometry.

5 Conclusion

The qualitative analytical investigation was carried out related to the temperature factor effect on separation flow physical features caused by a compression corner in the supersonic viscous flow. The numerical results of simulation the same flow based on the Navier–Stokes equations are also presented. It is shown that the separation zone length decreases as the temperature factor decreases. For high values of the compression corner in numerical investigations there were discovered vortices in the separation zone that were not observed before. These vortices effect considerably on heat exchange in the separation zones. The temperature factor effect on the pressure center position was investigated. It is shown that at small corner angles a temperature factor increase may deteriorate static stability of the vehicle, while at big angles it may improve static stability of the vehicle.

The work has been performed under the grant of RFBR (Russian Foundation for Basic Research) (projects No 07-08-000124 and 06-08-01558a)

References

1. Neiland, V. Ya., Kukanova, N. I., 1965, Investigation of flows with separation zones. Review of TsAGI, No. 129.
2. Lapin, Yu. V., Loytsianskii, L. G , Lun'kin, Yu. P., Neiland, V. Ya., Sychev, V. V., Tirskii, G. A., 1970, Mechanics of Viscous Liquids and Gases. Theory of Laminar and Turbulent Boundary Layers. Mechanics in USSR for Fifty Years. Vol. II, Nauka, Moscow.
3. Charwat, A. F., 1970, Supersonic Flows with Imbedded Separation Regions, in: Advances in Heat Transfer, Vol. 6. Academic, New York.
4. Chang, P. K., Separation of Flow. Pergamon, Oxford.
5. Chapman, D. R., 1951, An analysis of base pressure at supersonic velocities and comparison with experiment. NASA Rep., No 1051. pp. 23.
6. Korst, H. H., 1956, A theory for base pressure in transonic and supersonic flow. J. Appl. Mech., Vol. 23, No. 4, pp. 593–600.
7. Neiland, V. Ya., 1970, Asymptotic theory of plane steady supersonic flows with separation zones. Fluid Dynamics, No. 3, pp. 372.
8. Neiland, V. Ya., 1968, Supersonic viscous flow near a separation point. Abstracts of the 3-rd All-Union Congress on Theoretical and Applied Mathematics, Nauka, Moscow, pp. 224.
9. Neiland, V. Ya., 1969, Theory of laminar boundary layer separation in supersonic flow. Fluid Dynamics, No. 4, pp. 33.
10. Stewartson, K., Williams, P. G., 1969, Self-induced separation. Proc. Roy. Soc. London. Ser. A., Vol. 312, 1509, pp. 181–206.
11. Stewartson, K., 1970, On laminar boundary layers near corners//Quart J. Mech. Appl. Math., Vol. 23, No. 2. pp. 137–152.
12. Neiland, V. Ya., 1971, Flow behind the boundary layer separation point in a supersonic stream. Fluid Dynamics, No. 3, pp. 378.
13. Smith, F. T., Khorrami, A. F., 1991, The interactive breakdown in supersonic ramp flow. J. Fluid. Mech., Vol. 224, pp. 197–215.
14. Korolev, G. L., Gajjar, J. S. B., Ruban, A. I., 2002, Once again on the supersonic flow separation near a corner. J. Fluid Mech., Vol. 463, pp. 173–199.
15. Neiland, V. Ya., Bogolepov, V. V., Dudin, G. N., Lipatov, I. I., 2004, Asymptotic Theory of Supersonic Viscous Gas Flows. M.: Fizmatlit, pp. 456.
16. Neiland, V. Ya., Bogolepov, V. V., Dudin, G. N., Lipatov, I. I., 2007, Asymptotic Theory of Supersonic Viscous Gas Flows. Elsevier, Oxford, The Netherlands, pp. 536.
17. Hayes, W. D., and Probstein, R. F., 1959, Hypersonic Flow Theory. Academic, New York.
18. Egorov, I. V., Zaitsev, O. L., 1991, On an approach to the numerical solution of the two-dimensional Navier-Stokes equations by the shock capturing method. Journal of Computational Mathematics and Mathematical Physics. Vol. 31, No 2. pp. 286–299.
19. Babaev, I. Yu., Bashkin, V. A., Egorov, I. V., 1994, Numerical solution of the Navier-Stokes equations using variational iteration methods. Comp. Maths Math Phys., Vol. 34, No 11. pp. 1455–1462.
20. Bashkin, V. A., Egorov, I. V., Ivanov, D. V., 1997, Application of Newton's method to the calculation of internal supersonic separated flows. Zh. Prikl. Mekh. Tekhn. Fiz., Vol. 38, No 1, pp. 30–42.
21. Godunov, S. K., 1959, Mat. Sb., Vol. 47, pp. 271.
22. Roe, P. L., 1981, Aproximate Rieman Solvers, Parameter Vectors, and Difference Scheme. Journal Computation Physics, Vol. 43, pp. 357–372.
23. Kolgan, V. P. , 1972, Uch. Zap. Tsentr. Aerogidrodin. Inst., Vol. 3, No. 6, pp. 68.

24. Saad, Y., Shultz, M. H., 1986, GMRES: a generalized minimal residual algorithm for solving nonsymmetric linear systems. SIAM Journal of Scientific and Statistical Computing, No.7, pp. 856–869.
25. Gil'manov, A. N., 2000, Methods of Adaptive Meshes in Gas Dynamic Problems, I. Nauka, Fizmatlit, Moscow, pp. 247.
26. Anderson, D. A., Tannehill, J. C., Pletcher, R. H., 1984, Computational Fluid Mechanics And Heat Transfer. Hemisphere, New York.
27. Stemmer, C., Adams, N. A., 2004, Investigation of supersonic boundary layers by DNS, ECCOMAS 2004 Proceedings, Vol. II.